Journal of Power Sources 242 (2013) 646–655

Contents lists available at SciVerse ScienceDirect

Journal of Power Sources

journal homepage: www.elsevier.com/locate/jpowsour

Degradation mechanisms and mitigation strategies of metal cations in recycled fuel for direct methanol fuel cell membrane electrode assembly

Min-Jee Yang [a], Ka-Young Park [a], Ki-Beum Kim [a], Hyejung Cho [b], Hanshin Choi [c], Jun-Young Park [a,*]

[a] HMC, INAME, Green Energy Research Institute, Department of Nanotechnology and Advanced Materials Engineering, Sejong University, 98 Gunja-dong, Gwangjin-gu, Seoul 143-747, Republic of Korea
[b] Energy Lab, Samsung Electronics Co. Ltd., San 14, Nongseo-dong, Giheung-gu, Yongin-si, Gyeonggi-do 446-712, Republic of Korea
[c] Rare Metals Research Group, Korea Institute of Industrial Technology, Incheon 404-254, Republic of Korea

HIGHLIGHTS

- Investigated the effects of metal cations in the fuel stream of DMFC.
- Determined the main cause of MEA degradation in the fuel contamination.
- Investigated the critical concentration of metal cations in methanol fuel.
- Tested various novel methods for mitigating the influence of metal contaminants.

ARTICLE INFO

Article history:
Received 14 March 2013
Received in revised form
24 May 2013
Accepted 26 May 2013
Available online 5 June 2013

Keywords:
Direct methanol fuel cells
Ion-exchange resin
Fuel impurity
Mitigation
Membrane electrode assembly

ABSTRACT

Some metal contaminants, such as Al^{3+}, Ni^{+2}, Fe^{2+} and Cr^{3+}, are produced during reactions in heat exchangers, stacks, and other fuel/water management system components. Due to the gradual build-up of these contaminants generated in the system, direct methanol fuel cell (DMFC) membrane electrode assemblies (MEAs) deteriorate steadily with increasing operation time. Hence, this study systematically investigates the effects of metal cations by supplying various concentrations of metal solutions to the fuel stream at constant-current densities, with the aim of understanding the mechanism and influence of metal contamination on a DMFC MEA. Various electrochemical diagnostic techniques are used to determine the main cause of MEA degradation, including electrochemical impedance spectroscopy, electrode polarization, and methanol stripping voltammetry. In addition, the critical concentration of metal cations in methanol fuel is investigated for high DMFC MEA stability. Further, various novel methods for mitigating the influence of the metal contaminants on the performance of a DMFC are suggested and verified.

1. Introduction

Direct methanol fuel cells (DMFCs) have been considered as attractive mobile power devices due to their high energy density of fuel, rapid start-up, convenient refueling, and long operation time [1–3]. DMFCs have also several advantages, such as compact system design without a humidifier, low operation temperature, and environmental friendliness [4,5]. Over the last decade, many efforts have been made to improve the performance of DMFCs through advances in the design and components of membrane electrode assemblies (MEAs), such as the optimization of gas-diffusion layers (GDLs), the use of highly active catalyst materials, and the development of highly ionic conductive polymer electrolyte membranes with reduced methanol crossover [6–9]. Hence, state-of-the-art DMFC MEAs can compete with hydrogen polymer electrolyte membrane fuel cell (PEMFC) MEAs for mobile and portable applications.

Various studies on the long-term durability of DMFCs have been carried out to determine the main mechanisms of performance deterioration using various electrochemical and physiochemical

* Corresponding author. Tel.: +82 2 3840 3848; fax: +82 2 3840 4342.
E-mail address: jyoung@sejong.ac.kr (J.-Y. Park).

0378-7753/$ – see front matter © 2013 Elsevier B.V. All rights reserved.
http://dx.doi.org/10.1016/j.jpowsour.2013.05.141

analysis techniques [10–12]. Bae et al. [13] presented a general guideline for the accelerated degradation testing (ADT) of DMFC MEAs. Their methodology illustrated the estimation of MEA lifetime distribution under normal DMFC operating conditions. The long-term stability of MEAs, however, still remains an obstacle to the commercialization of DMFCs. In particular, the presence of impurities and reaction intermediates can negatively affect the long-term stability of a DMFC MEA.

To date, most research dealing with impurities has focused on gas impurities, which mainly come from reformed hydrogen and environmental air supplied directly by an internal air pump for the PEMFC system. There have been few reports regarding the effects of methanol fuel impurities and reaction intermediates for DMFC systems [14–17]. These products accumulate continuously in the circulating loop of diluted methanol with the water produced by the electrochemical reactions at the cathode as the DMFC operates, even though fresh methanol is supplied to the fuel mixing tank from a fuel cartridge to recover the original concentration of the solution. We previously investigated DMFC contamination sources and the electrochemical effect of recycled methanol fuel through physicochemical analysis of the reaction products generated by the DMFC system components [18]. Some contaminants are produced by reactions of the heat exchangers, stack, and other fuel/water management system components. According to inductively coupled plasma-atomic emission spectroscopy (ICP-AES) and gas chromatography–mass spectrometry (GC–MS) analyses, the recycled fuel contains some heavy metal cations, such as Al^{3+}, Ni^{+2}, Fe^{2+}, and Cr^{3+}, and organic contaminants, such as methyl formate and formic acid. Due to the gradual build-up of these intermediates and contaminants generated in the system, the DMFC MEAs deteriorated steadily with increasing operation time [19,20]. Systematic and comprehensive investigations of the electro/physicochemical poisoning effects of inorganic metal contaminants generated by DMFC system balance-of-plants (BOPs), such as Al^{3+}, Ni^{+2}, Fe^{2+} and Cr^{3+}, however, have been limited.

Hence, the primary objective of this work is to study the effect of the presence of stainless steel constituents in the fuel stream, such as Al^{3+}, Ni^{+2}, Fe^{2+}, and Cr^{3+}, on DMFC performance and short-term stability. We systematically investigate the effects of metal cations by supplying various concentrations of metal solutions to the fuel stream at constant-current densities, with the aim of understanding the mechanism and influence of metal contamination on a DMFC MEA. Various electrochemical diagnostic techniques are used to determine the main cause of MEA degradation, including electrochemical impedance spectroscopy (EIS), electrode polarization, and cyclic voltammetry (CV). To determine the ion-exchange capacity (IEC) of Nafion membranes, a postmortem diagnostic is conducted, including a base titration analysis of contaminated MEA samples. In addition, we propose a critical limiting concentration of impurities in methanol fuel for high DMFC MEA stability. Various novel methods for mitigating the impact of the reaction contaminants in the performance of DMFC system are suggested and verified.

2. Experimental

2.1. MEA preparations and contamination evaluations

MEAs were prepared from a Nafion membrane (perfluorosulfonate ionomer, Dupont, USA) with commercial Pt-Ru/C and Pt/C (Hispec, Johnson Matthey, UK) as the anode and cathode catalysts, respectively. The catalyst loadings for the anode and cathode were 4 and 2 mg cm^{-2}, respectively. Carbon paper (TGP-H-60, Japan) was used as a gas-diffusion layer (GDL) for both electrodes, and the active area of MEAs was 25 cm^2.

All of the electrochemical performance characteristics of the DMFCs were measured on a fuel cell test station (Scitech Inc., Korea) using single-cell hardware (Fuel Cell Technologies Inc., USA), as shown in Fig. 1. The bipolar plates were a triple serpentine-type flow-field design. Single-cell measurements were acquired at 65 °C in galvanostatic mode at a current density of 120 mA cm^{-2} for 8 h. Dry air was supplied to the cathode side at a flow rate of 163 ml min^{-1} under ambient pressure. A 1 M aqueous methanol solution was fed to the anode side at a flow rate of 0.932 ml min^{-1}. To investigate the effect of metal cations on the DMFC performance, the cell was fed with 1 M MeOH solution containing different concentrations of Cr^{3+} [$Cr(NO_3)_3 \cdot 9H_2O$ (98.5%, Alfa Aesar, USA)], Al^{3+} [$Al(NO_3)_3 \cdot 9H_2O$ (98%, Alfa Aesar, USA)], Fe^{3+} [$Fe(NO_3)_3 \cdot 9H_2O$ (99.99%, Sigma–Aldrich, USA)], and Ni^{2+} [$Ni(NO_3)_2 \cdot 6H_2O$ (99.9985%, Alfa Aesar, USA), $NiCl_2$ (98%, Alfa Aesar, USA) and $NiCO_3$ (99%, Alfa Aesar, USA)]. Various concentrations of metal contaminants of 1 μM (10^{-6} mol l^{-1}), 10 μM (10^{-5} mol l^{-1}), 100 μM (10^{-4} mol l^{-1}), 250 μM (2.5×10^{-4} mol l^{-1}), 500 μM (5.0×10^{-4} mol l^{-1}), 1000 μM (10^{-3} mol l^{-1}) were supplied to the anode of the DMFC MEA. The polarization curves of the MEAs were recorded before and after the procedure in constant-current density mode at 65 °C. Finally, the cell was flushed with deionized water for 2 h to remove metal cations.

Different methods for minimizing the impact or recovering the performance of a DMFC system were tested. First, ion-exchange resins (IERs, Amberject UP6150; Rohm & Haas, Germany, and SM210; Samyang, Korea) were installed at the anode inlet of the DMFC MEA, as shown in Fig. 1. The results of contamination evaluations were compared to those obtained without the IER. Second, a method of reactivating the MEA was carried out by supplying fully humidified H_2 (anode; 913 sccm) and air (cathode; 3620 sccm) with applied voltage cycling (50 cycles) in a range of 0.9–0.3 V for 8 h, as is performed in polymer electrolyte membrane fuel cells (PEMFCs) for activating the MEA. Third, H_2SO_4 solution (0.5 and 1.0 M) was fed to the anode with 1 M MeOH (anode, 0.932 ml min^{-1}) and air (cathode, 163 sccm), and the cell was operated at a current density of 120 mA cm^{-2} for 8 h. Fourth, the poisoned MEA was purged by 1.0 M H_2SO_4 solution (anode, 3 ml min^{-1}) and N_2 gas (cathode, 200 sccm) for 1 h, and then washed with deionized water for 5 min. The polarization curves of the MEAs were measured at 65 °C after each mitigation procedure for the recovery of the cell performance.

2.2. Electrochemical analysis

Extensive electrochemical analyses were carried out to closely examine the MEA degradation mechanisms by contamination of metal cations dissolved in MeOH fuel. Electrochemical impedance

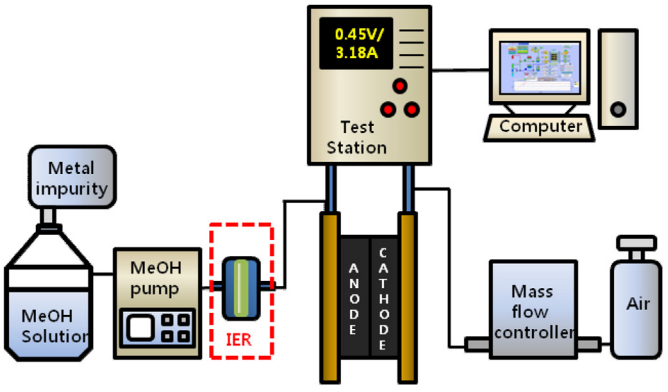

Fig. 1. Impurity test setup for the effect of metal-cation fuel contaminations on DMFC performance.

spectroscopy (EIS) measurements were carried out using an EIS analyzer coupled with an SP-150 Potentiostat (Bio-Logic SAS, France). All EIS measurements were carried out before and after MEA contamination experiments. Dry air (cathode) and 1 M MeOH (anode) were supplied at flow rates of 163 sccm and 0.932 ml min^{-1}, respectively. EIS data was obtained at 120 mA cm^{-2} and 65 °C using frequency ranging from 10 kHz to 0.01 Hz. The EIS of a cell anode was measured in galvanostatic mode at 120 mA cm^{-2} by the feeding humidified H_2 (150 sccm) and 1 M MeOH (0.932 ml min^{-1}) to the cathode and anode, respectively. The cathode impedance was obtained by subtracting the anode impedance from the total impedance.

The methanol stripping voltammetry (MSV) technique was used to measure the electrochemical surface area (ESA) of the anode in the potential range of 0–0.6 V at a scan rate of 20 mV s^{-1} at 65 °C. For the MSV measurement, 1 M methanol was fed to the anode while holding the potential at 0.45 V for 1 h. The anode was then flushed with deionized water (2 ml min^{-1}), and humidified hydrogen (150 sccm) was fed to the cathode.

For the polarization measurements, the cathode potentials were obtained from the sum of the anode polarization and internal ohmic resistance (IR)-corrected cell voltage after the IR was measured by the EIS. Anode polarization was evaluated in galvanodynamic polarization mode with a scan rate of 20 mA s^{-1} at 65 °C. The anode and cathode compartments acted as the working and counter electrodes (dynamic hydrogen reference electrode, DHE), respectively.

To determine the total ion-exchange capacity (IEC) of the Nafion membranes, acid-base titration method was used before and after impurity tests using a 1000 μM metal-cation solution. The dried membrane (3 × 3 cm) was immersed in 20 ml of NaCl aqueous solution and equilibrated for 24 h using a magnetic bar. Phenolphthalein indicator solution was dropped into the aqueous solution, and 20 mM NaOH was then transferred to the solution, and each sample was titrated until the endpoint was reached, as indicated by the persistence of a light pink color. Finally, the IEC values of contaminated MEAs were calculated from the volume of solution required to titrate the sample.

3. Results and discussions

3.1. Influence of metal-cation impurities

The effect of metal cations on the overall performance of a DMFC was first investigated by introducing $M(NO_3)_3$ (M = Al, Fe and Cr) and $M^*(NO_3)_2$ (M^* = Ni) to the anode methanol fuel of an fuel cell operating at 65 °C. Fig. 2 shows the effect of the metal nitrates added to the 1 M MeOH solutions at various concentrations on the constant-current density mode of 120 mA cm^{-2} for 8 h. In the beginning, the DMFC was operated with uncontaminated MeOH fuel at a constant-current density to achieve stable performance. The cell voltage dropped negligibly with Ni^{+2}, Fe^{3+}, Al^{3+}, and Cr^{3+} impurities in the solution at zero mol l^{-1}. After switching to fuel containing the impurity, however, it was clearly shown that the current density gradually decreased at all metal solutions with increasing operation time and metal concentrations. In particular, the current density significantly decreased in a few hours when the fuel was changed to the MeOH fuel containing 100 μM (10^{-4} mol l^{-1}) of metal impurities. The decay ratios of the cell voltage were 0.012, 0.041, 0.057, and 0.061 V h^{-1} for Fe^{3+}, Ni^{+2}, Cr^{3+} and Al^{3+} cations at concentrations of 1000 μM. The DMFC performance was restored to some extent in the low-impurity-level methanol solution when the anode of the cell was flushed with distilled water for 2 h after the measurement, but could not be recovered entirely.

The order of the contamination effect on the cell voltage was $Fe^{+3} < Ni^{2+} < Cr^{3+} < Al^{3+}$ cations, as shown in Fig. 3. The decay ratios of Fe^{3+}, Ni^{+2}, Cr^{3+}, and Al^{3+} were 19.9, 58.74, 61.27, and 70.11% at a metal impurity concentration of 1000 μM. The lowest degradation ratio of the Fe^{3+} impurity might be due to the Pt/C catalyst with dissolved Fe in the electrode being more active for the oxygen reduction reaction (ORR) than Pt/C catalysts. It has been reported that Pt–Fe catalysts lead to higher net ORR currents than Pt catalysts, and restrain methanol oxidation reaction [21–25]. Pt–Ni alloy catalysts also previously exhibited enhanced electrocatalytic activities for ORR with a lower activity of methanol oxidation [26]. The decay ratio of Ni^{2+} impurity, however, was high at a concentration of 1000 μM. This indicates that Ni^{2+} impurity has a significant impact on other MEA components such as proton exchange membrane or anode. The dominant degradation mechanisms will be analyzed in the forthcoming section. The degradation patterns of contaminated cells on the cell voltage were similar to each other. By comparing the cell voltages, it appears that the rate of cation contamination strongly depends on the metal-cation concentration. A higher concentration of metal impurities corresponded to the observation of a higher poisoning rate. The cell voltage steadily decreased until 100 μM and dropped markedly afterward. Thus, the critical concentration of metal-cation impurities is identified as 100 μM for the performance degradation of a DMFC MEA.

The effects of anion species such as NO_3^-, Cl^-, and CO_3^- were investigated under DMFC operating conditions using Ni^{2+}-based impurity solutions. Fig. 4 shows the cell voltage variations of DMFC MEAs with time, applying Ni^{2+} impurity solutions mixed with 1 M MeOH fuel to the anode. The DMFC MEA impurity test was performed at 120 mA cm^{-2} and 65 °C for 8 h. It was observed that the cell voltage dropped with increasing impurity concentration. Fig. 5 shows a comparison of the performance decay ratio obtained using fuel containing Ni^{2+}-based anion impurity solutions for the anode feed. By comparing the cell voltages for various anion solutions, it was observed that the degradation rates were similar. With a high Ni impurity concentration (1000 μM), the CO_3^- solution showed relatively smaller performance degradation than NO_3^- and Cl^-. The performance decay rate was increased in the order of CO_3^- (30.34%), NO_3^- (58.74%), and Cl^- (59.38%). The onset of performance decay appeared at an impurity concentration of 250 μM. This drop in cell voltage could not be recovered to its initial performance level after changing to normal operation.

3.2. Poisoning mechanisms by metal impurities

3.2.1. Polarization curve analysis

Significant developments have been made in recognizing contamination sources and understanding the impact of contaminants on PEMFC performance through experimental and modeling approaches. In terms of fundamental understanding, three major effects can be identified in the MEA during the contamination process: poisoning of the electrode catalysts, increase in the resistance of the polymer electrolyte membrane and catalyst layer ionomer, and mass transfer problems due to changes in hydrophobicity of the gas-diffusion layer (GDL) and microporous layer (MPL) [27–30]. We believe that a similar explanation is also applicable to the study of DMFCs.

To investigate the poisoning mechanisms of the DMFC MEA, polarization curves were measured after DMFC operation in the absence and presence of various concentrations of metal impurities. MEA performance was measured in a fresh 1 M MeOH solution and dry air with a flow rate corresponding to a stoichiometry of 3, after each contamination test run at 65 °C. The performance drop of contaminated MEAs by Ni^{+2}, Fe^{3+}, Al^{3+}, and Cr^{3+} cations

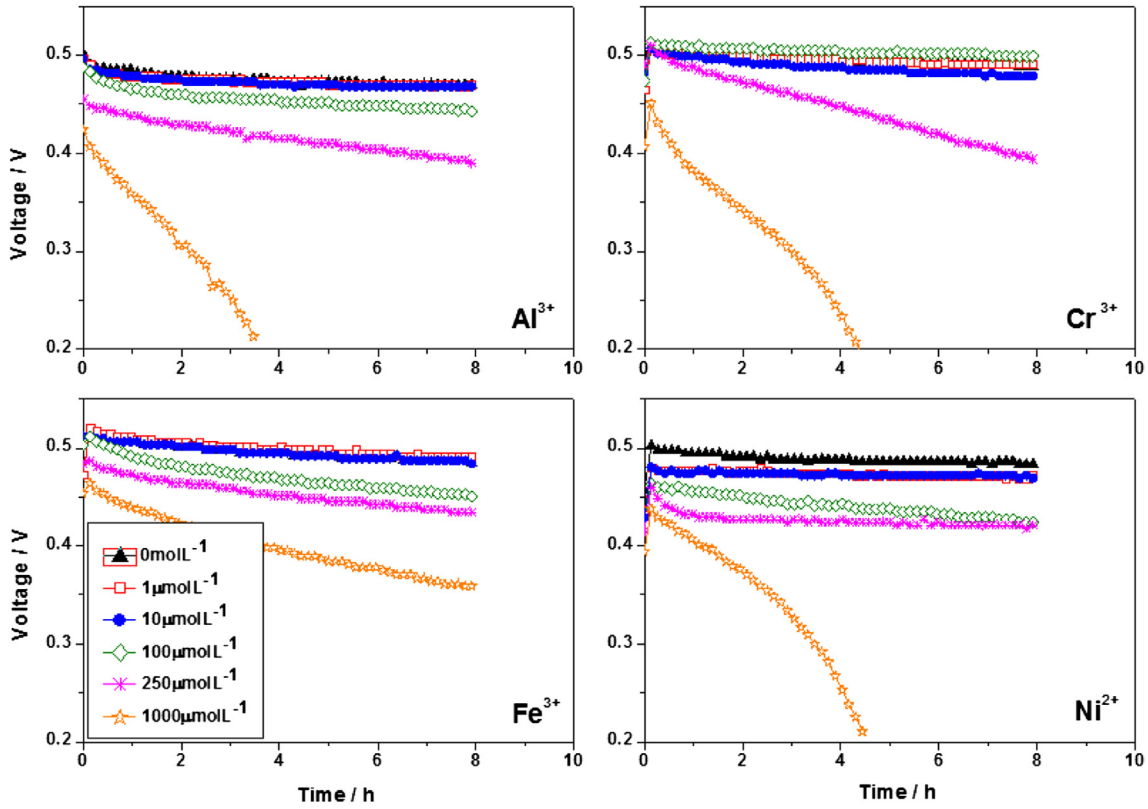

Fig. 2. Constant-current discharge curve of the DMFC in various concentrations of metal cations for 8 h, at 120 mA cm^{-2} and 65 °C.

was quite significant after 250 μM impurity tests, when no visible degradation was observed for the MEA containing no metal cations, as illustrated in Fig. 6. All metal impurities from methanol fuel streams, even at a level of 100 μM, can cause a degradation in cell performance, especially in high current density regions. This indicates that metal cations affect the mass transfer of methanol in the anode and the water removal and mass oxygen transfer in the cathode [31,32]. In addition, current-voltage curves gradually shifted downward as metal impurities were added. The voltage losses became deeper with prolonged exposure to metal cations, due to accumulation of the cations on the MEA over time.

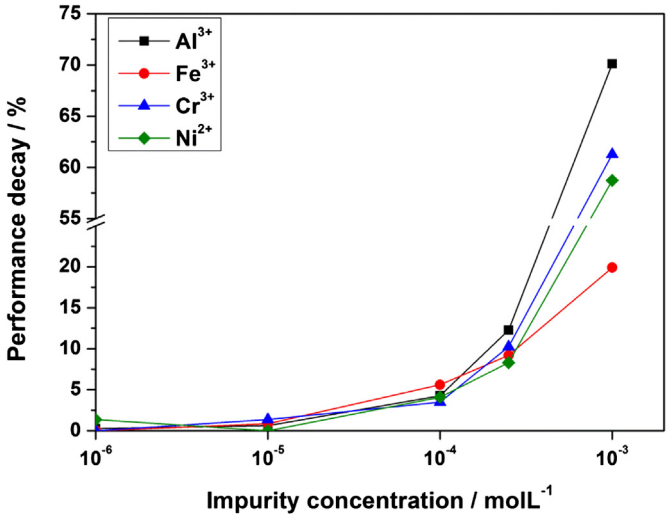

Fig. 3. Degradation ratio of the DMFC running with various metal cations at 120 mA cm^{-2} and 65 °C.

This behavior is clear indication of the increase in resistance of the polymer membrane by the adsorbed metal cations on the DMFC MEA. It is believed that metal cations reduce the proton conductivities of both the Nafion membrane and the anode catalyst ionomer layer. Cationic ions such as alkali metals, alkaline earth metals, and transition metals have been reported to directly affect the transport properties of the electrolyte membrane, because many cationic species have a high affinity for the sulfonic groups in Nafion membranes [28–30,33]. Previous results indicated that the diffusion and transport characteristics of protons and water are directly affected by the exchange between cationic ions and protons. Chen et al. [21] and Okada et al. [34] predicted that cationic impurities would result in serious membrane degradation, due to the formation of oxygen radicals caused by the reaction with hydrogen peroxide according to reaction (1) [35,36]:

$$Me^{3+} + HO_2^{\cdot} \rightarrow Me^{2+} + H^+ + O_2 \quad (1)$$

Fig. 7 shows the IEC value of a Nafion membrane before and after impurity tests at a 1000 μM concentration of metal cations. The IEC values decreased significantly from 0.94 to 0.459 (Ni^{2+}), 0.552 (Al^{3+}), 0.458 (Cr^{3+}) and 0.634 (Fe^{+3}) meq g^{-1}. These results confirmed that metal cations are affected by exchanging with protons inside the membrane directly, thus resulting in decreased proton conductivity of membrane. Furthermore, metal cation crossover from the anode to the cathode could also contaminate the cathode of DMFC MEAs. The adsorption of metal cations on the platinum surface caused a slight drop in performance in the catalyst activation polarization region of the *I–V* curves. This phenomenon may be explained by the formation of metal–hydroperoxy complexes in the cathode catalyst layer, as suggested by Chen et al. [21,37].

$$Me^{3+} + H_2O_2 + H_2O \rightarrow [Me(III)–(OH)(O_2H)]^+ + 2H^+ \quad (2)$$

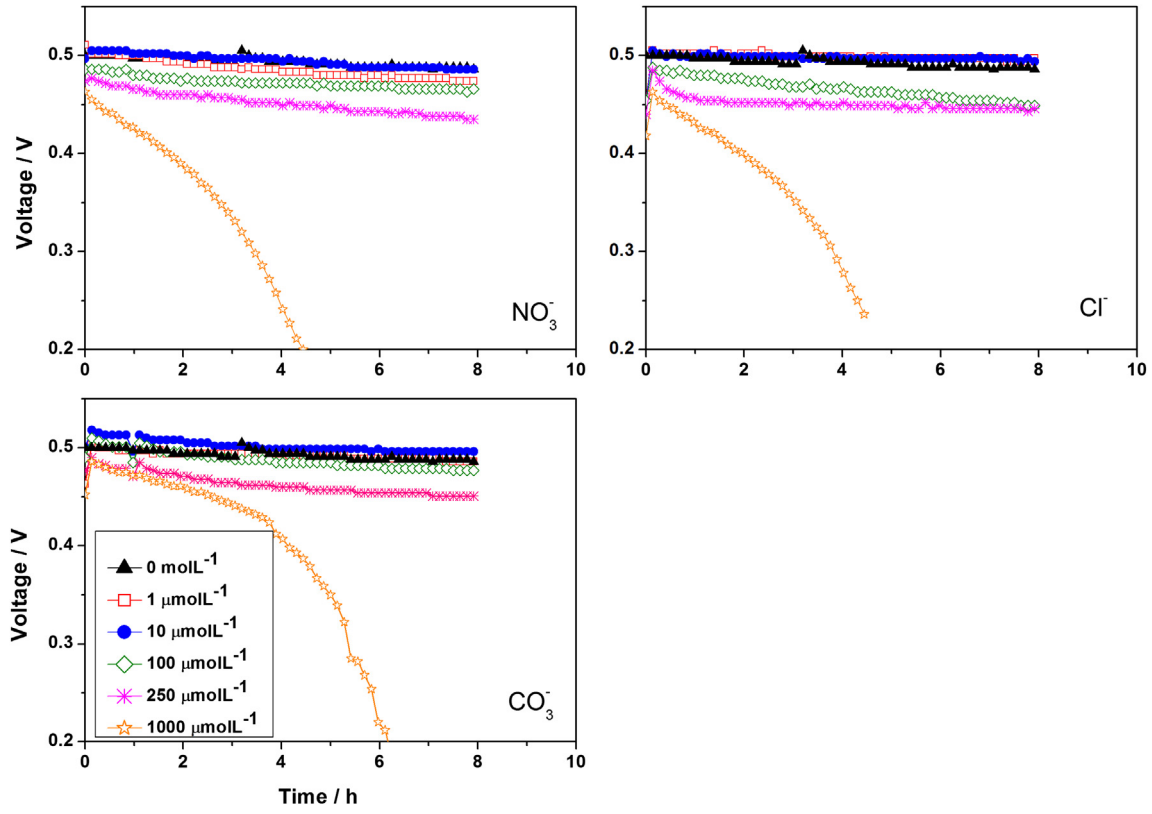

Fig. 4. Constant-current discharge curve of the DMFC in various anion species for 8 h, at 120 mA cm^{-2} and 65 °C.

These metal–hydroperoxy complexes were relatively stable, and could not be removed completely by flushing the cell with deionized water.

The IR-corrected anode and cathode polarization curves of the cells before and after the contamination test were measured to identify the main causes of the experimental results with regard to performance decay, and the result is given in Fig. 8. The onset potential for methanol oxidation reaction increased somewhat with the increase in the concentration of metal cations. DMFC MEAs broadly commence the generation of a current density of more than 0.28 V (DHE), irrespective of the kinds of metal impurities. Significant mass-transport losses, however, were observed with an anode polarization potential of up to 0.4 V (DHE) after each contamination test run at 1000 μM concentrations of Ni^{+2}, Fe^{3+}, Al^{3+} and Cr^{3+} cations. The order of the contamination effect on the anode polarization loss was $Fe^{+3} < Cr^{3+} < Al^{3+} < Ni^{2+}$. This was not in agreement with the results of the overall cell degradation ($Fe^{+3} < Ni^{2+} < Cr^{3+} < Al^{3+}$), as presented in Fig. 3. This observation supports the explanation that Ni^{+2} has a strong negative effect on the catalytic oxidation of methanol [26]. This may have resulted from the Ni^{+2} affecting the electrochemical properties of the anode, primarily by exchanging with protons of the membrane and ionomer, thus resulting in decreased ionic conductivity.

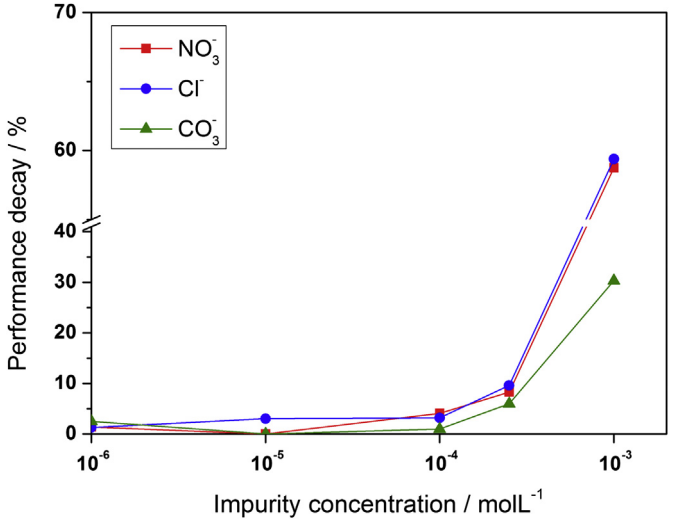

Fig. 5. Degradation ratio of the DMFC running with various anion species at 120 mA cm^{-2} and 65 °C.

The cathode polarization voltage is approximately equal to the sum of the terminal voltage and the polarization voltage of the anode. The cathode potentials tested with metal impurities showed significant changes in ohmic and concentration polarization, while those of the cell tested without metal impurities steadily decreased, maintaining values of 0.75–0.85 V at the current density onset (Fig. 8). In particular, in the middle and high current regions (e.g. >0.1 A cm^{-2}), where the ohmic and concentration polarizations are dominant, the impact of metal impurities was significant in the polarization curves of the cathode in operation with Al^{+3} and Cr^{+3} when the anode and cathode polarizations were compared among MEAs. This suggests that metal impurities affected the mass transfer of methanol in the anode and oxygen in the cathode for the water removal [33–38]. Metal cations decreased the proton conductivity of the catalyst ionomer layer. In addition, this change in ohmic polarization is related to membrane failure, as mentioned earlier. Furthermore, there might be a high flux of metal cation crossover reaching the cathode from the anode, which results in increasing the overpotential for oxygen reduction by poisoning of the catalyst.

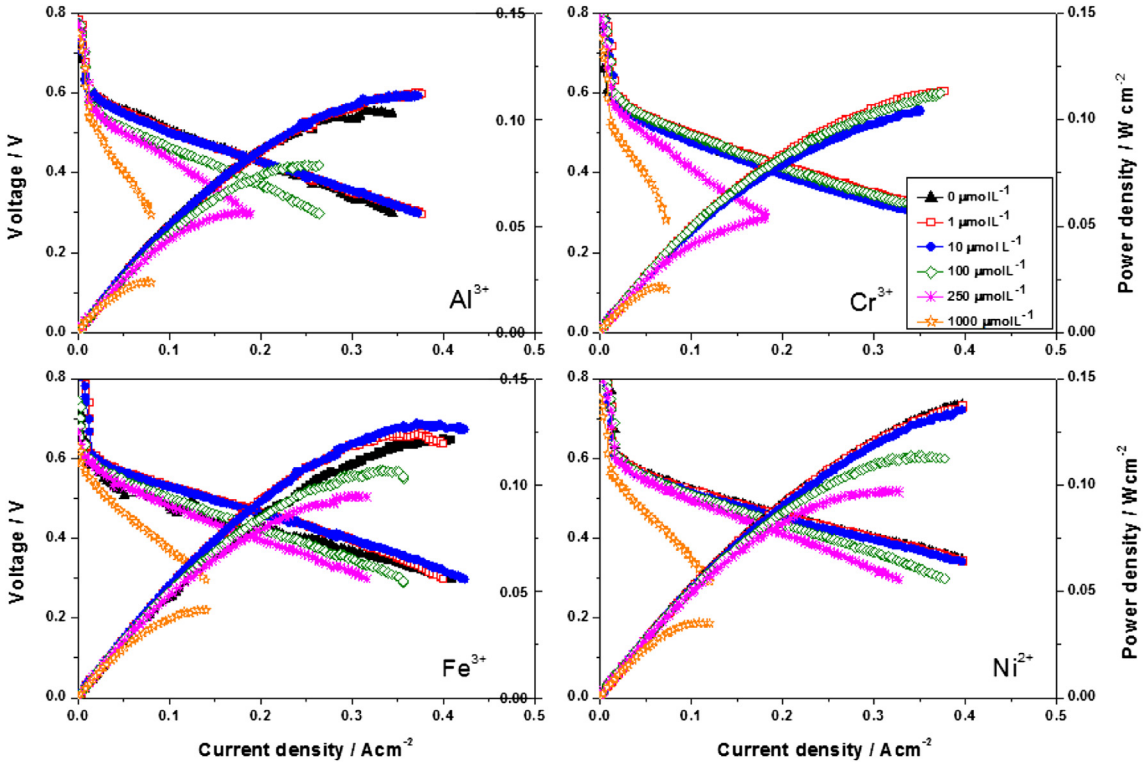

Fig. 6. Polarization and power density curves measured after DMFC operation in the absence and presence of various concentrations of metal impurities.

3.2.2. MSV and EIS analysis

The impact of metal cations was further analyzed by methanol stripping voltammetry (MSV) technique [39,40] and electrochemical impedance spectroscopy (EIS) measurements. MSV measurements were carried out with a scan rate of 20 mV^{-1} at 65 °C, and showed the degradation of the electrochemical surface area (ESA) of the carbon-supported Pt electrode (Fig. 9) by metal impurities. MSV curves indicate that ESAs are drastically reduced after each contamination test run with 1000 μM concentrations of Ni^{+2}, Fe^{3+}, Al^{3+}, and Cr^{3+} cations, since the methanol desorption peaks explain the characteristics of the electrocatalytic active surface availability of an electrode. In particular, DMFC operation with Ni^{2+} cation (1000 μM) resulted in more significant ESA reduction compared to that of metal cations, which is in agreement with the results of anode polarization curves. The decreased ESA is due to the combined effect of increased interfacial resistance between the catalyst particles and the ionomers and Pt catalyst degradation through the adsorption of metal cations on the Pt surface [41,42].

The EIS of each MEA was performed to provide further evidence of these explanations, using single cell and anode measurements under galvanostatic control at 120 mA cm^{-2}, 65 °C, and with 1 M MeOH. The cathode impedance was determined by subtracting the anode impedance from the total impedance. Fig. 10(a) shows the total impedance plot before and after impurity experiments with 1000 μM concentrations of Ni^{+2}, Fe^{3+}, Al^{3+}, and Cr^{3+} cations.

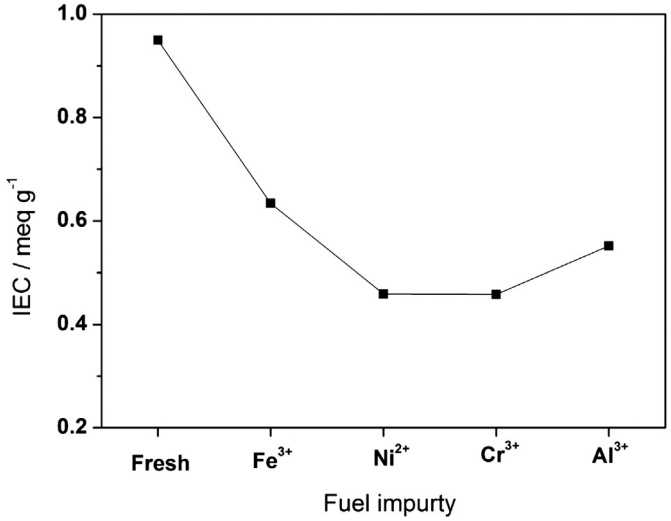

Fig. 7. IEC values of Nafion membrane before and after impurity tests with 1000 μM of metal cations.

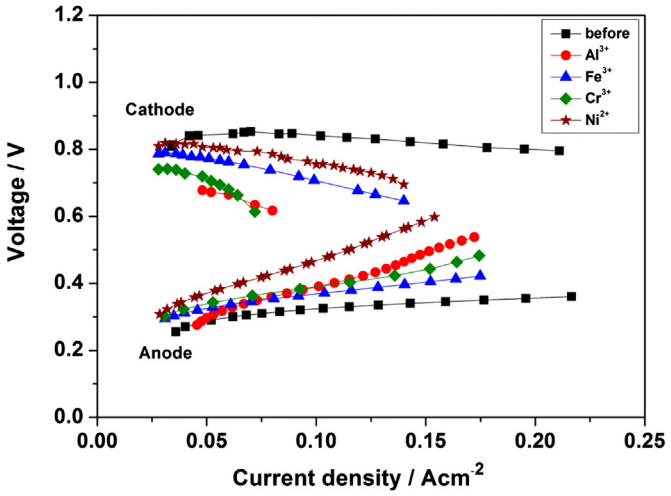

Fig. 8. IR-corrected anode and cathode polarization curves of the cells during the metal cation impurity tests.

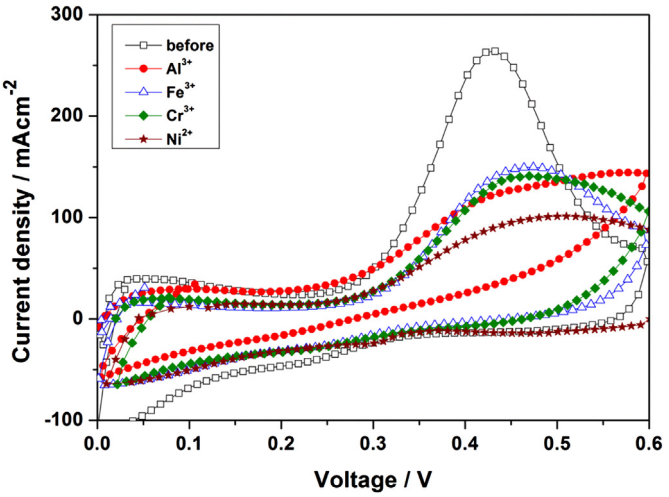

Fig. 9. MSV curves of the anode of MEAs during the metal-cation impurity tests.

The ohmic resistance, indicated by the real intercept with the real axis at high frequency, increased significantly from 0.09 to 0.16 (Fe^{3+}), 0.44 (Ni^{2+}), 0.47 (Cr^{3+}), and 0.48 (Al^{3+}) $\Omega\,cm^2$ for methanol and air cells. This means that metal cations affected the water flux and proton conductivity inside the membrane through the displacement of protons with metal cations directly, leading to severe Nafion degradation. In addition, the second arc of contaminated MEAs increased significantly, which is in agreement with the results presented in polarization curves, when compared to the first arc in the total impedance (Fig. 10(a)). The increase of the second semicircle is due to the mass-transport limitation at low frequency, since the mid- and low-frequency intercepts correspond to the charge transfer and mass transfer resistance of the cell. A high flux of metal cation crossover reaching the cathode from the anode also resulted in a limitation in the mass transport for oxygen reduction by poisoning the catalyst and ionomers in the cathode, as mentioned in the previous section. This phenomenon was confirmed by cathode EIS curves, as shown in Fig. 10(b). Furthermore, the charge transfer resistance (the second arc in the EIS curve) in the MEA contaminated with Al^{3+} and Cr^{3+} also increased significantly, as shown in Fig. 10(a). This might have been because the Pt/C catalyst with Al^{3+} and Cr^{3+} dissolved in the methanol fuel became more deactivated for oxygen reduction than those with other metals dissolved (Fe^{3+} and Ni^{2+}), inhibiting the formation of hydroperoxy complexes. In contrast, the degradation trend of contaminated MEAs in anode impedance looked similar in Fig. 10(c). Ni^{2+} and Al^{3+} impurity, however, showed the largest degradation in the anode impedance, including the ohmic resistance of the cell. This result matched with the results of anode polarization and MSV curves of metal cations. In summary, it was observed that metal-cationic ions affected the membrane and cathode ionomer, primarily by exchanging with protons of the membrane/ionomer, including anode kinetic losses, resulting in considerable performance loss.

3.3. MEA degradation mitigation

3.3.1. Ion-exchange resins

Previously, we introduced that ion-exchange resins (IERs) for a DMFC system mitigate the impurity effects on the DMFC performance, because IERs can easily take up specific impurity ions due to the pore structures developed on the surface [18]. IERs in a DMFC system trapped contaminants effectively and released H^+

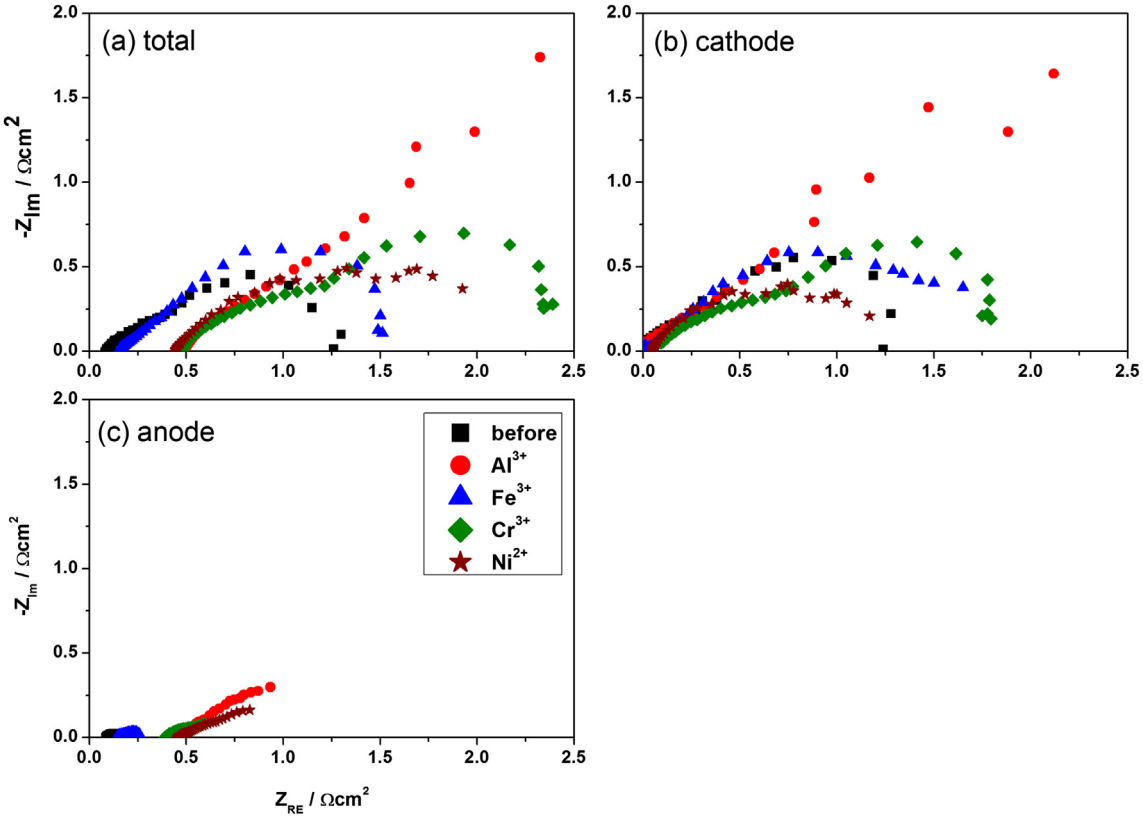

Fig. 10. EIS patterns of the MEAs tested at 65 °C and 120 mA cm^{-2} after the metal-cation impurity tests: (a) total; (b) cathode; (c) anode impedance spectra.

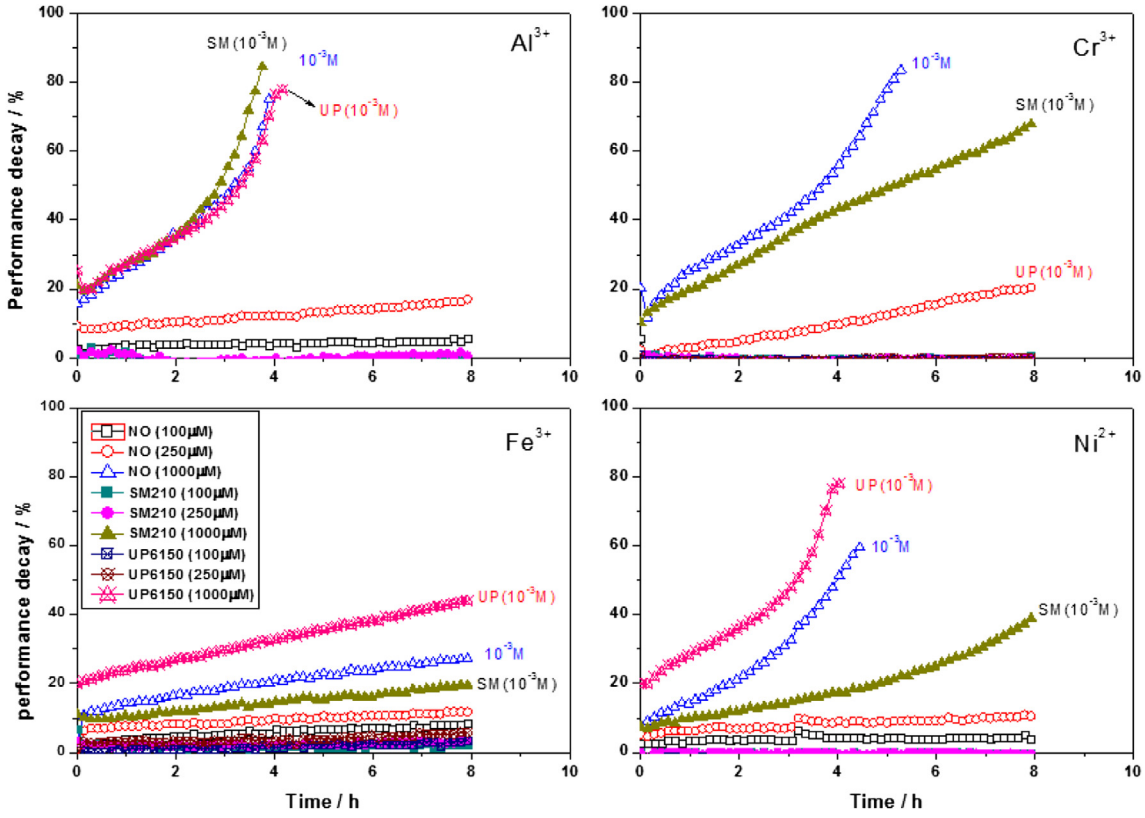

Fig. 11. Voltage decay curves during the contamination test with and without IERs (SM210 and UP6150); 65 °C, 120 mA cm^{-2} and 8 h.

and OH^- into the methanol fuel, thereby minimizing the MEA decay by fuel contaminants. The degree, capacity, and kind of IER in the ion-exchange effect, however, need to be analyzed further. Therefore, a fully regenerated mixed bed of cation and anion exchange resins was installed at the inlet of a stack anode intended for use in high-purity fuel systems through reverse osmosis, as shown in Fig. 1. Two types of IERs (UP6150 and SM210) were tested with the DMFC system in constant-current mode (123 mA cm^{-2}) for 8 h.

Fig. 11 shows the degradation ratio of MEA performance in the DMFC with and without IERs by the metal nitrates added to the 1 M MeOH solutions at various concentrations (100, 250 and 1000 μM). Interestingly, the stack performance without an IER was decreased remarkably by fuel contaminants, whereas the degradation of the MEA was mitigated by the IER during the DMFC operation. The decay ratios of the DMFC MEA without IERs were 21, 18, 11, and 11% in Cr^{3+}, Al^{3+}, Fe^{3+}, and Ni^{2+} solutions (250 μM), respectively, while the IERs showed negligible performance degradation in Cr^{3+}, Al^{3+}, and Ni^{2+} (250 μM), as shown in Fig. 12. In addition, operation with Fe^{3+} cations showed performance loss less than 5%. This was due to the removal of contaminants in the recycled fuel by the IERs, as expected. The IERs exchanged all metal cations with H^+, thus resulting in the generation of pure methanol fuel. In addition, the ion-exchange effects of the UP6150 and SM210 IERs against fuel contamination were similar in the DMFC system. The performance degradation, however, became severe with metal-cation concentrations more than 1000 μM, even with an IER. This means that IERs were ineffective for exchanging metal cations at these higher concentrations. As a reference, the ion-exchange capacities (initial resistivities) of SM210 and UP6150 were 0.45 eq l^{-1} (5.0 MΩ cm) and 1.0 eq l^{-1} (16.0 MΩ cm), respectively. A high concentration (>1000 μM) of Cr^{3+} and Al^{3+} cations were particularly detrimental to the performance of the DMFC systems with an IER.

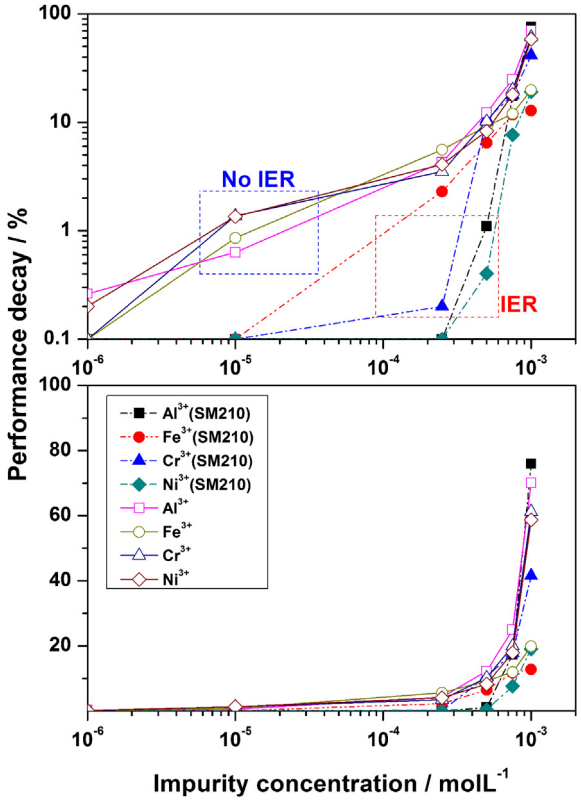

Fig. 12. Decay ratios of the DMFC running in various metal cations with and without IERs (SM210); 65 °C, 120 mA cm^{-2} and 8 h.

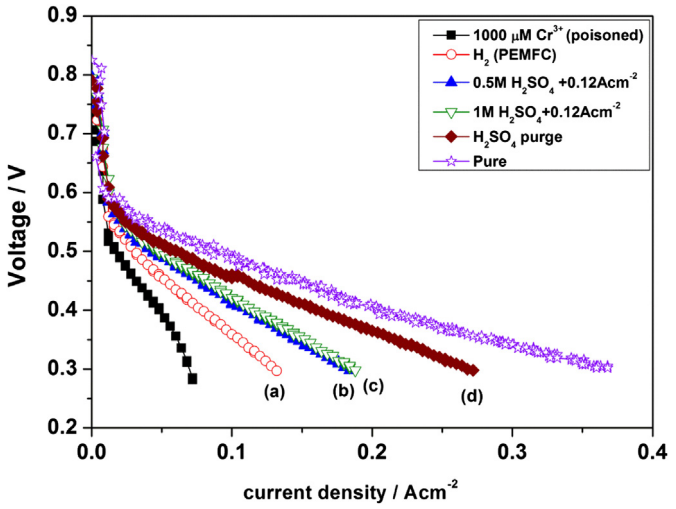

Fig. 13. Performance recovery of contaminated DMFC MEAs through various reactivation methods.

3.3.2. Reactivation methods

To recover the performance of MEAs degraded by fuel impurities, a recovery strategy should also be developed. Various reactivation methods were applied to significantly poisoned MEAs using reducing gas purging (hydrogen), solution soaking (dilute H_2SO_4, DI water), and current impulse (high constant current). Fig. 13 illustrates the polarization curve of the cell after the constant-current operation of 120 mA cm^{-2} for 8 h with the continued supply of methanol containing 1000 μM Cr^{3+}. In order to reactivate the contaminated DMFC MEA, deionized water was first fed to both electrodes for 8 h. However, there was negligible effect on the recovery of cell performance. Further, the anode was purged by 10 M MeOH for 2 h, and a slight improvement in cell performance was achieved (data not shown).

Secondly, a method of reactivating MEAs was also used to recover a contaminated membrane and electrodes by supplying fully humidified H_2 (anode) and air (cathode) with applied voltage cycling in the range of 0.9–0.3 V for 8 h, as polymer electrolyte membrane fuel cells (PEMFCs) perform for activating through the hydration of an MEA. The cell performance, however, showed no significant recovery after 8 h of reactivation, as shown in Fig. 13(a).

Thirdly, H_2SO_4 solution (0.5 and 1.0 M) was fed into the anode with 1 M MeOH (anode) and air (cathode), and the cell was operated at a current density of 120 mA cm^{-2} for 8 h. This reactivation method was more effective for recovering the cell performance to some extent than the PEMFC activation method by H_2 purging, but no further improvement was achieved (Fig. 13(b) and (c)).

Lastly, a recuperation process was conducted by purging a poisoned MEA with 1.0 M H_2SO_4 solution (anode) and N_2 gas (cathode) for 1 h, followed by washing with deionized water for 5 min. The cell performance was clearly recovered through the dilute H_2SO_4 treatment, as shown in Fig. 13(d). Even though the DMFC MEA performance was still somewhat lower than the initial performance, this process was the most effective, in that there was a high recovery rate of cell performance with no auxiliary components such as IERs.

4. Conclusions

The impact of metal impurities such as Cr^{3+}, Al^{3+}, Fe^{3+} and Ni^{2+} in methanol fuel on the performance of DMFC MEAs was investigated. The cell performance was directly affected by the concentration of metal cations in 1 M MeOH fuel. The performance of DMFC MEAs was markedly degraded with increasing impurity concentration from 1 μM to 1000 μM. In particular, the current density significantly decreased with methanol fuel containing 100 μM of metal impurities. According to various electrochemical analyses, such as anode/cathode polarization curves, EIS, and MSV measurements, it was determined that metal impurities affected the mass transfer of methanol in the anode and oxygen in the cathode for the water removal. In addition, metal cations decreased the proton conductivity of the catalyst ionomer layer by exchanging with protons of the membrane/ionomer. Furthermore, a high flux of metal cation crossover reaching the cathode from the anode resulted in increasing the overpotential for oxygen reduction by poisoning the catalyst.

As a mitigation strategy to lessen the effects of impurities on the DMFC performance, IERs were introduced at the inlet of the DMFC stack anode for use in high-purity fuel systems through reverse osmosis. The IERs showed negligible performance degradation with Cr^{3+}, Al^{3+}, Fe^{3+} and Ni^{2+} ($\leq$250 μM) cations. This is because the IERs exchanged all metal cations with H^+, resulting in the removal of contaminants in the recycled fuel. In addition, the 1.0 M H_2SO_4 solution purge process was the most effective for recovering the performance of a contaminated MEA in that there was a high recovery rate of cell performance with no auxiliary components such as IERs.

Acknowledgments

This study was supported by the New & Renewable Energy project of a Korea Institute of Energy Technology Evaluation and Planning (KETEP) grant funded by the Korean Ministry of Knowledge Economy (No. 2011T100200280), the Fundamental R&D Program for Core Technology of Materials funded by the Ministry of Knowledge Economy (#10037289, Development of Highly Active and Sustainable Hybrid Catalysts), and the Fusion Research Program for Green Technologies through the National Research Foundation of Korea (NRF, #2011-0004428).

References

[1] P. Gislon, G. Monteleone, P. Prosini, Int. J. Hydrogen Energy 34 (2009) 929–937.
[2] W. Qian, D.P. Wilkinson, J. Shen, H. Wang, J. Zhang, J. Power Sources 154 (2008) 202–213.
[3] S.K. Kamarudin, F. Achmad, W.R.W. Daud, Int. J. Hydrogen Energy 34 (2009) 6902–6916.
[4] Z. Guo, A. Faghri, J. Power Sources 160 (2006) 1142–1155.
[5] A.S. Patil, T.G. Dubois, N. Sifer, E. Bostic, K. Gardner, M. Quah, C. Bolton, J. Power Sources 136 (2004) 220–225.
[6] T. Shimizu, T. Momma, M. Mohamedi, T. Osaka, S. Sarangapani, J. Power Sources 137 (2004) 277–283.
[7] A. Santasalo-Aarnio, M. Borghei, I.V. Anoshkin, A.G. Nasibulin, E.I. Kauppinen, V. Ruiz, T. Kallio, Int. J. Hydrogen Energy 37 (2012) 3415–3424.
[8] D. You, Y. Lee, C. Pak, H. Cho, H. Chang, G. Lee, K.-Y. Park, J.-Y. Park, Int. J. Hydrogen Energy 36 (2011) 5096–5103.
[9] F. Liu, C.-Y. Wang, Electrochim. Acta 52 (2006) 1417–1425.
[10] J.-Y. Park, S.-J. Song, J.-H. Lee, J.-H. Kim, H. Cho, Int. J. Hydrogen Energy 35 (2010) 7982–7990.
[11] J. Liu, Z. Zhou, X. Zhao, Q. Xin, G. Sun, B. Yi, Phys. Chem. Chem. Phys. 6 (2004) 134–137.
[12] M.K. Jeon, K.R. Lee, K.S. Oh, D.S. Hong, J.Y. Won, S. Li, S.I. Woo, J. Power Sources 158 (2006) 1344–1347.
[13] S.J. Bae, S.-J. Kim, S. Um, J.-Y. Park, J.-H. Lee, H. Cho, Int. J. Hydrogen Energy 35 (2010) 4606–4621.
[14] F. Jing, M. Hou, W. Shi, J. Fu, H. Yu, P. Ming, B. Yi, J. Power Sources 166 (2007) 172–176.
[15] J.M. Moore, P.L. Adcock, J.B. Lakeman, G.O. Mepsted, J. Power Sources 85 (2004) 254–260.
[16] X. Jie, Z.-G. Shao, J. Hou, G. Sun, B. Yi, Electrochim. Acta 55 (2010) 4783–4788.
[17] S.T. Ali, Q. Li, C. Pan, J.O. Jensen, L.P. Nielsen, P. Møller, Int. J. Hydrogen Energy 36 (2011) 1628–1636.
[18] J.-Y. Park, K.-Y. Park, K.B. Kim, Y. Na, H. Cho, J.-H. Kim, J. Power Sources 196 (2011) 5446–5452.
[19] J.-W. Guo, X.-F. Xie, J.H. Wang, Y.-M. Shang, Electrochim. Acta 53 (2008) 3056–3064.

[20] B.R. Padhy, R.G. Reddy, J. Power Sources 153 (2006) 125–129.
[21] W. Chen, Q. Xin, G. Sun, S. Yang, Z. Zhou, Q. Mao, P. Sun, Electrochim. Acta 52 (2007) 7115–7120.
[22] K. Scott, W. Yuan, H. Cheng, J. Appl. Electrochem. 37 (2007) 21–26.
[23] V. Baglio, A.S. Aricò, A. Stassi, C. D'Urso, A. Di Blasi, A.M. Castro Luna, V. Antonucci, J. Power Sources 159 (2006) 900–904.
[24] W. Li, W. Zhou, H. Li, Z. Zhou, B. Zhou, G. Sun, Q. Xin, Electrochim. Acta 49 (2004) 1045–1055.
[25] A.K. Shukla, R.K. Raman, N.A. Choudhury, K.R. Priolkar, P.R. Sarode, S. Emura, R. Kumashiro, J. Electroanal. Chem. 563 (2004) 181–190.
[26] H. Yang, C. Coutanceau, J.-M. Léger, N. Alonso-Vante, C. Lamy, J. Electroanal. Chem. 576 (2005) 305–313.
[27] X. Cheng, Z. Shi, N. Glass, L. Zhang, J. Zhang, D. Song, Z.-S. Liu, H. Wang, J. Shen, J. Power Sources 165 (2007) 739–756.
[28] M. Shi, F.C. Anson, J. Electroanal. Chem. 425 (1997) 117–123.
[29] H.L. Yeager, A. Steck, J. Electrochem. Soc. 128 (1981) 1880–1884.
[30] M.J. Kelly, B. Egger, G. Fafilek, J.O. Besenhard, H. Kronberger, G.E. Nauer, Solid State Ionics 176 (2005) 2111–2114.
[31] H. Kim, S.J. Shin, Y.G. Park, J. Song, H.T. Kim, J. Power Sources 160 (2006) 440–445.
[32] J.-Y. Park, J.-H. Kim, Y. Seo, D.-J. Yu, H. Cho, S.J. Bae, Fuel Cells 12 (2012) 426–438.
[33] T. Okada, N. Nakamura, M. Yuasa, I. Sekine, J. Electrochem. Soc. 144 (2006) 2744–2750.
[34] T. Okada, G. Xie, Y. Tanabe, J. Electroanal. Chem. 413 (1996) 49–65.
[35] M. Inaba, T. Kinumoto, M. Kiriake, R. Umebayashi, A. Tasaka, Z. Ogumi, Electrochim. Acta 51 (2006) 5746–5753.
[36] A. Pozio, R.F. Silva, M. De Francesco, L. Giorgi, Electrochim. Acta 48 (2003) 1543–1549.
[37] T.-C. Jao, S.-T. Ke, P.-H. Chi, G.-B. Jung, S.-H. Chan, Int. J. Hydrogen Energy 35 (2010) 6941–6949.
[38] J.-Y. Park, M.A. Scibioh, S.-K. Kim, H.-J. Kim, I.-H. Oh, T.G. Lee, H.Y. Ha, Int. J. Hydrogen Energy 34 (2009) 2043–2051.
[39] A.S. Aricò, V. Baglio, A. Di Blasi, E. Modica, P.L. Antonucci, V. Antonucci, J. Electroanal. Chem. 557 (2003) 167–176.
[40] M. Carmo, V.A. Paganin, J.M. Rosolen, E.R. Gonzalez, J. Power Sources 142 (2005) 169–176.
[41] A.K. Shukla, M. Neergat, P. Bera, V. Jayaram, M.S. Hegde, J. Electroanal. Chem. 504 (2001) 111–119.
[42] E. Antolini, J. Mater. Sci. 38 (2003) 2995–3005.